ACS chemical biology

Articles

pubs.acs.org/acschemicalbiology

Fluorinated *N,N*-Dialkylaminostilbenes Repress Colon Cancer by Targeting Methionine *S*-Adenosyltransferase 2A

Wen Zhang,[†,⊥,⍰] Vitaliy Sviripa,[∥,†,⍰] Xi Chen,[†,⊥] Jiandang Shi,[†,⊥] Tianxin Yu,[†,⊥] Adel Hamza,[§] Nicholas D. Ward,[†] Liliia M. Kril,[†,⊥] Craig W. Vander Kooi,[†] Chang-Guo Zhan,[§] B. Mark Evers,[‡,⊥] David S. Watt,[∥,†,⊥] and Chunming Liu*[,†,⊥]

[†]Department of Molecular and Cellular Biochemistry, [‡]Department of Surgery, College of Medicine, [§]Department of Pharmaceutical Sciences, College of Pharmacy, [∥]Center for Pharmaceutical Research and Innovation, and [⊥]Markey Cancer Center, University of Kentucky, Lexington, Kentucky 40506-0509, United States

Supporting Information

ABSTRACT: Methionine *S*-adenosyltransferase 2A (MAT2A) is the catalytic subunit for synthesis of *S*-adenosylmethionine (SAM), the principal methyl donor in many biological processes. MAT2A is up-regulated in many cancers, including liver cancer and colorectal cancer (CRC) and is a potentially important drug target. We developed a family of fluorinated *N,N*-dialkylaminostilbene agents, called FIDAS agents, that inhibit the proliferation of CRC cells *in vitro* and *in vivo*. Using a biotinylated FIDAS analogue, we identified the catalytic subunit of MAT2A as the direct and exclusive binding target of these FIDAS agents. MAT2B, an associated regulatory subunit of MAT2A, binds indirectly to FIDAS agents through its association with MAT2A. FIDAS agents inhibited MAT2A activity in SAM synthesis, and depletion of MAT2A by shRNAs inhibited CRC cell growth. A novel FIDAS agent delivered orally repressed CRC xenografts in athymic nude mice. These findings suggest that FIDAS analogues targeting MAT2A represent a family of novel and potentially useful agents for cancer treatment.

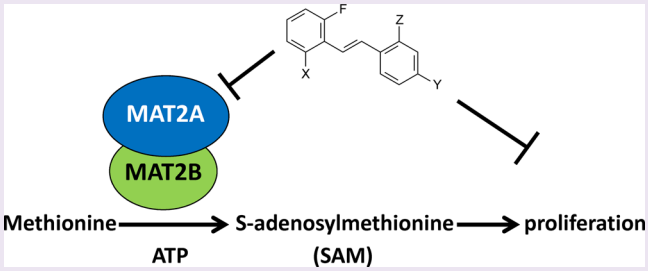

Colorectal cancer (CRC) is the second leading cause of cancer-related mortality in the United States.[1] In developing new therapeutic agents for CRC treatment, we focused initially on compounds related to the naturally occurring stilbenes (Figure 1A). Several of the natural products in this family inhibit the expression of several oncogenes and repress the proliferation of CRC cells[2−4] but only at relatively high levels and with a plethora of off-target effects. We suspect that these polyphenolic natural products undergo redox reactions that lead to numerous metabolites affecting many biological targets. To prevent these redox reactions and to optimize exclusively anticancer activity, we developed a family of fluorinated *N,N*-dialkylaminostilbenes (FIDAS agents) that lack any hydroxy or methoxy groups. These FIDAS agent inhibited CRC cell proliferation and repressed growth of human CRC xenografts in athymic nude mice with no notable effects on body weight.[4]

To identify the binding partner of these biologically active FIDAS agents and confirm the anticancer selectivity of these agents, we synthesized and evaluated a number of biotinylated analogues (**FIDAS-6**, **7**, and **8**, Figure 1A) related to the most active **FIDAS-3** agent (**4r** in previous study)[4] and identified **FIDAS-8** as ideally suited to the purpose at hand in that it displayed activity comparable to that of **FIDAS-3**. Using this **FIDAS-8** agent, we purified a single binding protein that we identified as the catalytic and regulatory subunits of methionine *S*-adenosyltransferase 2A and 2B (MAT2A and MAT2B, respectively). MAT (E.C.2.5.1.6) catalyzes the synthesis of *S*-adenosylmethionine (SAM) from ATP and L-methionine.[5] In mammals, there are three types of methionine *S*-adenosyltransferases, MATI/III and MATII. MATI and III are tetramers or dimers, respectively, of the α1 catalytic subunit (MAT1A). They are expressed principally in adult liver.[6] MATII, on the other hand, is a heterotrimer consisting of two catalytic α2 subunits (MAT2A) and a regulatory β subunit (MAT2B) of type II methionine *S*-adenosyltransferases. MAT2A and MAT2B are widely expressed in proliferating cells and cancers.[7−10] The product of MAT2A, namely SAM, is the principal methyl donor of many biological processes, including DNA methylation, protein methylation, and creatine and polyamine synthesis. In the study reported here, we characterize the interaction between FIDAS agents and MAT2A and the implications for this interaction in cancer repression.

RESULTS AND DISCUSSION

Novel FIDAS Agents and Their Biotinylated Analogues Inhibit CRC Cell Proliferation. To improve the potency and bioavailability of FIDAS agents as potential

Received: October 2, 2012
Accepted: January 29, 2013
Published: January 30, 2013

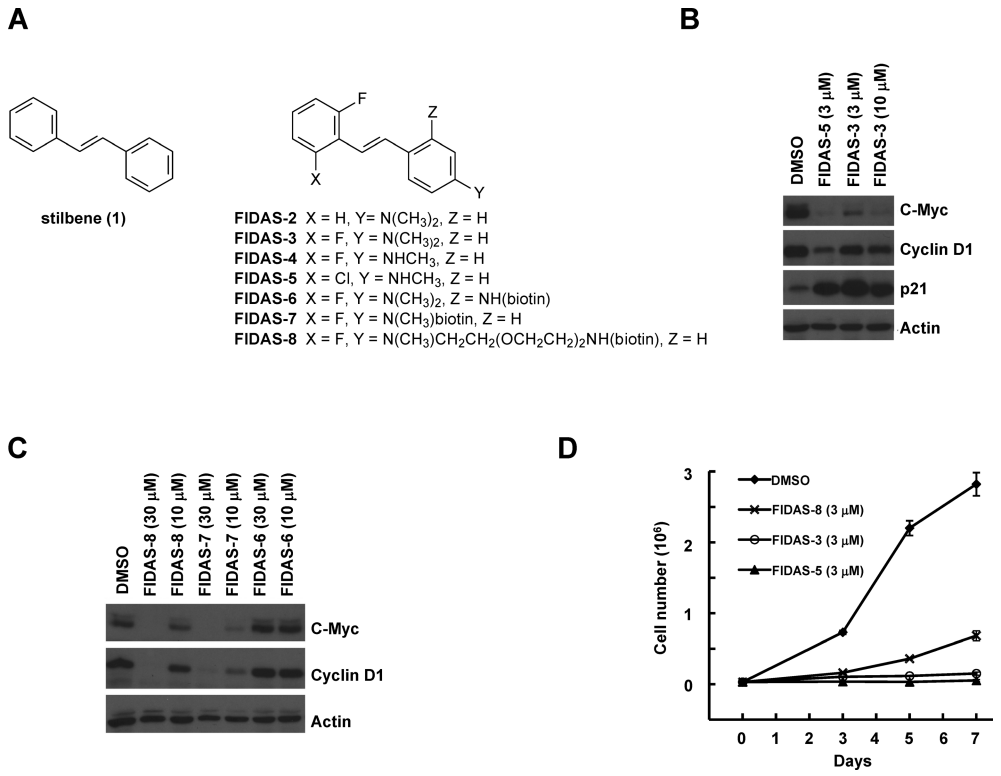

Figure 1. Identification of biologically active FIDAS surrogates and their biotinylated counterparts. (A) Structures of stilbene (**1**), **FIDAS-2**−**5** and biotinylated **FIDAS-6**−**8**. (B) **FIDAS-3** and **FIDAS-5** inhibited the expression of c-Myc and cyclinD1 in LS174T CRC cells. The expression was analyzed by Western blotting. The levels of cell cycle inhibitor, $p21^{WAF1/CIP1}$, were increased. (C) Biotinylated FIDAS analogues inhibited c-Myc and cyclinD1. LS174T cells were treated with biotinylated FIDAS analogues. The expression of c-Myc and cyclinD1 were analyzed by Western blotting. (D) FIDAS analogues repressed the proliferation of LS174T colon CRC cells. The viable cells were analyzed using a Cell Viability Analyzer (Beckman Coulter, Vi-Cell XR). Presented data are means ± SD from 3 independent experiments.

therapeutic agents, we performed a structure−activity relationship (SAR) study using gene expression and CRC cell proliferation as readouts.[4] **FIDAS-3** emerged as one of the most promising of the candidates in that it possessed suitable potency and a reasonable half-life *in vivo* (351 ± 180 min).[11] The activities of **FIDAS-3** and several other analogues, namely, **FIDAS-4** and **FIDAS-5** (Figure 1A), were tested in LS174T CRC cells (Figure 1B). **FIDAS-3** and **FIDAS-5** inhibited the expression of oncogenes, c-Myc and CyclinD1, at concentrations in the 3−10 μM range and induced the expression of cell cycle inhibitor, $p21^{WAF1/CIP1}$. **FIDAS-4** and several other FIDAS agents have similar activity.

To identify the molecular target, we synthesized biotinylated **FIDAS-6**, **7**, and **8** agents based on the SAR studies described above (Figure 1A and Supplementary Methods) and treated LS174T CRC cells with each of them. **FIDAS-7** and **FIDAS-8**, but not **FIDAS-6**, inhibited the expression of c-Myc and CyclinD1 (Figure 1C) at a level at least comparable to that of the lead compound, **FIDAS-3**. **FIDAS-8** had improved solubility and possessed a longer spacer than the spacer **FIDAS-7**. Because the longer spacer separated the biotin moiety and the stilbene part of **FIDAS-8** and made the biotin probe more accessible to both the target(s) and the streptavidin beads (Figure 1A), it was used in further studies.

We also analyzed the effects of **FIDAS-3**, **FIDAS-5**, and **FIDAS-8** on the proliferation of CRC cells. The FIDAS agents, including the biotinylated **FIDAS-8**, significantly inhibited the proliferation of LS174T cells (Figure 1D). These results establish that the biotinylated analogue, **FIDAS-8**, possesses the biological activities of nonbiotinylated FIDAS agents and is a valid surrogate for the purification and identification of the binding proteins of FIDAS analogues.

Identification of MAT2A as the Binding Target of FIDAS Agents. The utilization of biotin-labeled molecules for the isolation and identification of protein targets is well established. We empirically determined the optimal spacer length between the two termini by analyzing various spacers between the FIDAS agent and biotin (Figure 2A). We established, through the synthesis of other stilbenes possessing the linker but lacking the biotin heterocycle or by testing the covalently attached linker and biotin alone, that the activity in **FIDAS-8** resided in the stilbene part and not in the biotin or the linker part of these molecules. The FIDAS compounds also exhibited strong fluorescence under UV light that facilitated the binding and eluting conditions for biotin-FIDAS and streptavidin beads. LS174T cell lysates collected from 100 15-cm plates were incubated with streptavidin beads with or without **FIDAS-8**. The interacting proteins were eluted with 2.5 mM D-biotin. The purified samples were separated by 4−12% gradient SDS-PAGE and analyzed by silver staining (Figure 2B). Only two specific protein bands were apparent, and the proteins were identified and analyzed by mass spectrometry methods. These two bands were MAT2A and MAT2B that were identified unambiguously by both MALDI-TOF/TOF and LC−MS/MS methods.

Since MAT2A and MAT2B are two subunits of the MATII heterotrimer, we next determined which of the two subunits directly interacts with FIDAS agents. We purified GST-tagged

dx.doi.org/10.1021/cb3005353 | *ACS Chem. Biol.* 2013, 8, 796−803

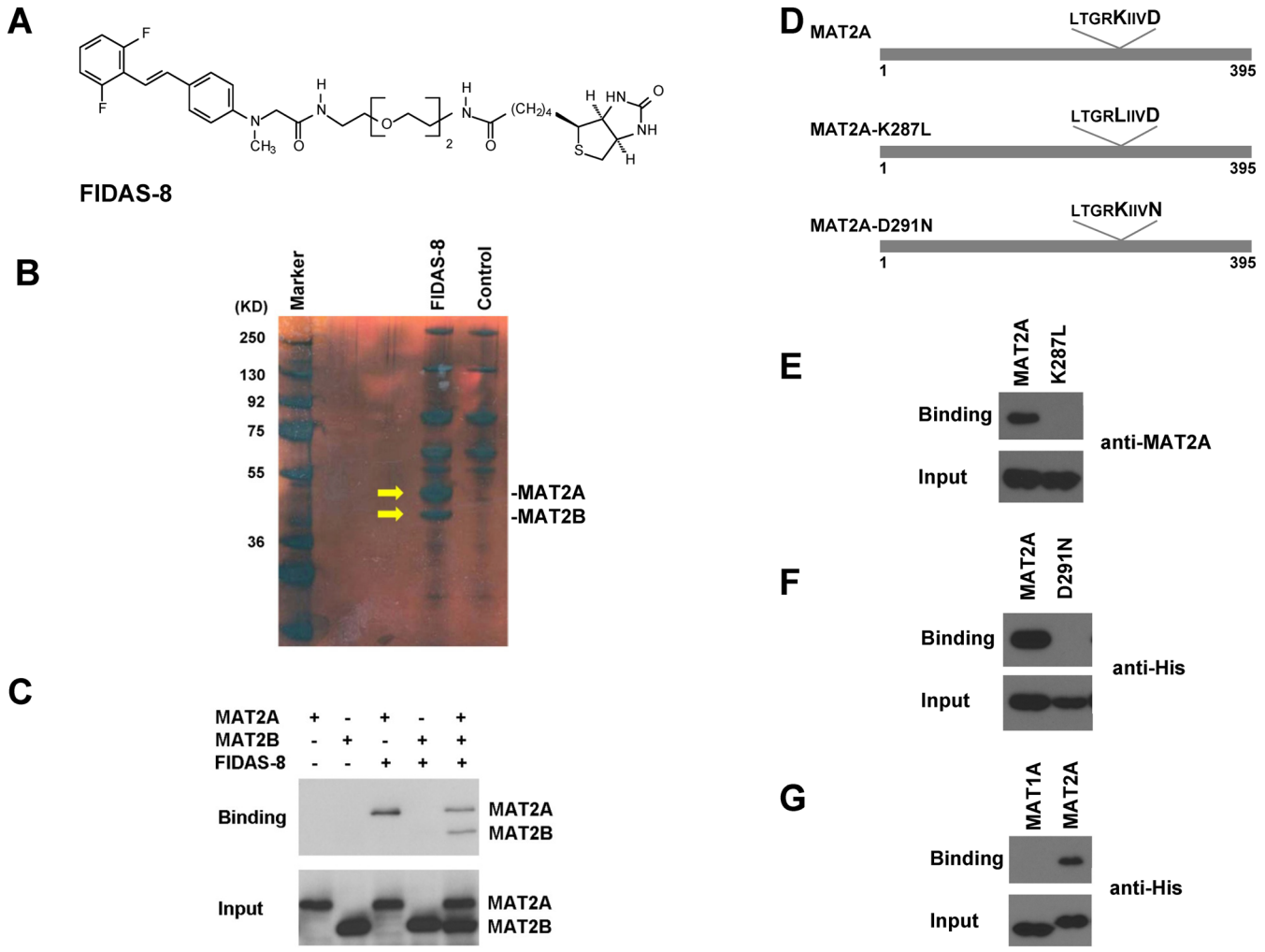

Figure 2. Identification of MAT2A as a binding target of FIDAS agents. (A) Structure of biotinylated **FIDAS-8** used for affinity purification. (B) Analysis of **FIDAS-8** binding proteins by silver staining. LS174T cell lysates were incubated with or without **FIDAS-8** and pulled down with streptavidin beads. The proteins were eluted with 2.5 mM D-biotin and separated by a 4−12% SDS-PAGE gel. (C) **FIDAS-8** directly interacted with MAT2A. GST-MAT2A and GST-MAT2B fusion proteins were expressed and purified from *E. coli*. These proteins were incubated with streptavidin beads with or without biotinylated **FIDAS-8.** The binding proteins were eluted with 2.5 mM D-biotin and analyzed by Western blotting with an anti-GST Ab. (D) Schematic MAT2A constructs. (E and F) Western blot showing that Lys287 and Asp291 in MAT2A are involved in FIDAS binding. (G) Western blot showing MAT2A, but not MAT1A, binds **FIDAS-8**.

MAT2A and MAT2B from *E. coli*. GST-MAT2A and GST-MAT2B proteins were incubated with **FIDAS-8**. The binding proteins were pulled down with streptavidin beads and analyzed by Western blotting with anti-GST Ab. We found that MAT2A directly binds biotinylated **FIDAS-8**, and MAT2B binds **8** indirectly through its association with MAT2A (Figure 2C).

The crystal structures of rat and *E. coli* MAT proteins have been described.[12,13] Several key residues conserved among different species are required for the binding of the substrates, L-methionine and ATP, or the product, SAM. To analyze the interaction between MAT2A and FIDAS agents, we generated several deletions and point mutations. We found that the point mutation K287L (Figure 2D), which has been proposed to be a key residue for MAT activity,[12,13] abolished **FIDAS-8** binding (Figure 2E). Another mutation, D291N, also abolished the binding (Figure 2F). We also tested the binding between **FIDAS-8** and MAT1A and found that **FIDAS-8** only binds MAT2A but not MAT1A (Figure 2G), consistent with the report that SAM selectively inhibits MAT2A,[14] but not MAT1A. These results further suggest that SAM and the FIDAS agents may bind to the same domain of MAT2A.

We performed a fluorescent anisotropy assay that relied on the fluorescent character of **FIDAS-3**.[4] The addition of MAT2A to **FIDAS-3** caused a significant increase in anisotropy, thereby demonstrating a significant increase in rotational time and direct binding (Figure 3A). Since SAM is a feedback inhibitor of MAT2A,[14] and SAM and its analogues have been used for MAT2A inhibition and cancer repression, we performed a competition assay using **FIDAS-3**, SAM, and purified MAT2A protein. Addition of SAM results in a dose-dependent decrease in **FIDAS-3** anisotropy toward that of the unbound molecule, suggesting a direct competitive binding of **FIDAS-3** to the active site of MAT2A. Since methionine also binds the active site of MAT, we performed a similar fluorescent anisotropy assay using methionine. We found that the interaction between MAT2A and **FIDAS-3** was inhibited by 5 μM methionine (Figure 3B), suggesting that methionine competes with FIDAS agents for MAT2A binding.

dx.doi.org/10.1021/cb3005353 | *ACS Chem. Biol.* 2013, 8, 796−803

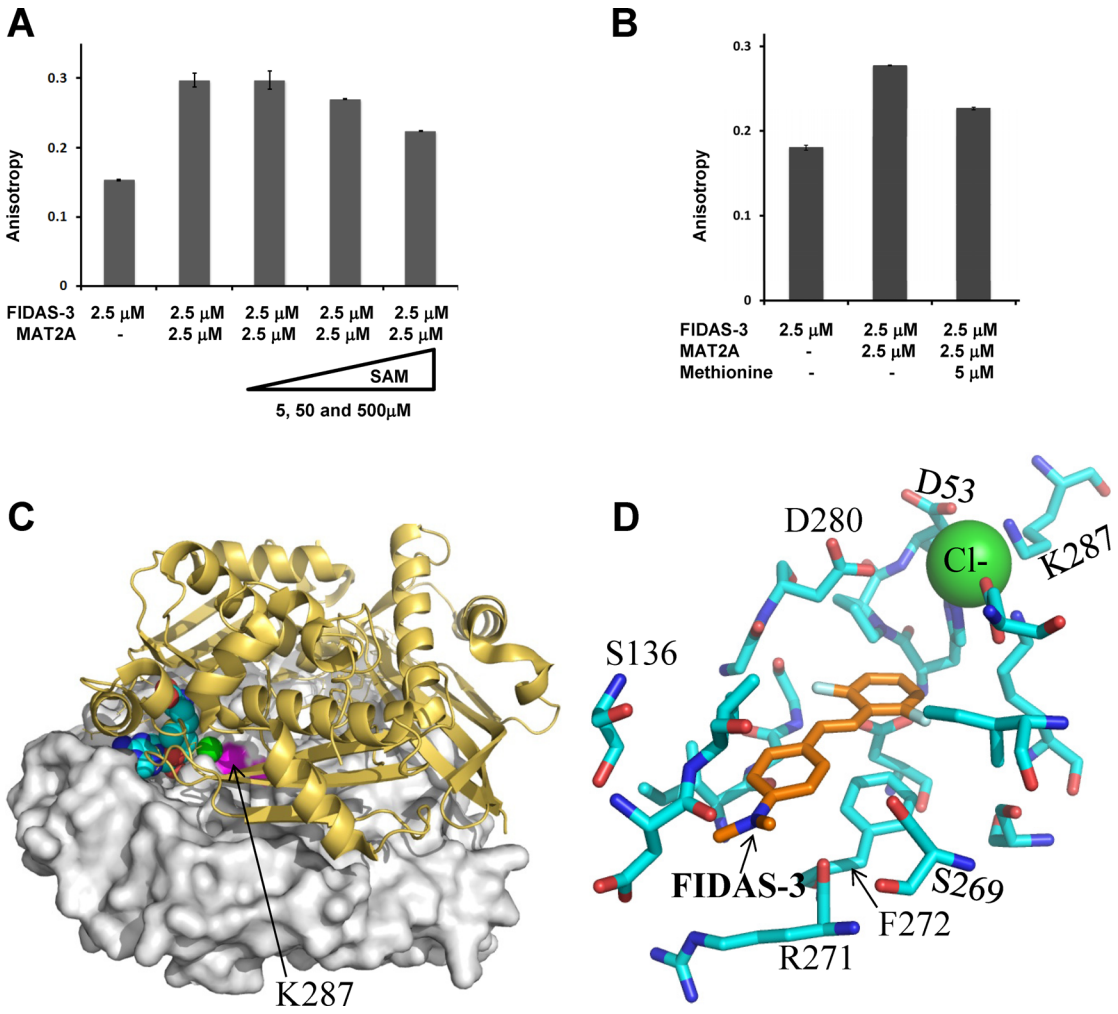

Figure 3. Interaction between FIDAS agents and MAT2A. (A) **FIDAS-3** competed with SAM for MAT2A binding. Fluorescence anisotropy was utilized to monitor the binding of **FIDAS-3** to MAT2A, because **FIDAS-3** has strong fluorescence under UV light.[4] **FIDAS-3** (2.5 μM) was measured alone and in combination with purified MAT2A (2.5 μM) along with increasing amounts of SAM (5, 50, 500 μM). Presented data are means ± SD from 3 independent experiments. (B) **FIDAS-3** competed with L-methionine for MAT2A binding. Fluorescence anisotropy of **FIDAS-3** (2.5 μM) was measured alone and in combination with purified MAT2A (2.5 μM) with or without 5 μM L-methionine. Presented data are means ± SD from 3 independent experiments. (C) The binding of SAM with MAT2A dimer based on the molecular docking and MD simulation. One MAT2A subunit is displayed as the solvent surface area (gray); the second MAT2A subunit is shown in gold ribbon. The binding pocket clearly lies at the interface of these two subunits with SAM displayed as space-filling spheres and chloride ion as a green sphere, and the position of K287 residue is colored in magenta. (D) The binding of **FIDAS-3** in the SAM-binding site of the dimeric MAT2A structure based on the molecular docking and MD simulation.

Binding Model of FIDAS-3 with MAT2A Dimer. Molecular docking and molecular dynamics (MD) were performed to determine the protein−ligand binding structures. As shown in Figure 3C, the SAM-binding site is located in a pocket formed at the interface between two α2 subunits of the MAT2A complex (PDB code: 2P02). The MD-simulated MAT2A-**FIDAS-3** complex structure revealed a stable binding mode for the ligand in the SAM-binding pocket of MAT2A (Figure 3D). The **FIDAS-3** scaffold is in close proximity to the chloride ion and makes $\pi-\pi$ interaction with the phenyl ring of F272 side chain. The superimposition of the binding site of the MAT2A-SAM crystal structure on that of MAT2A-**FIDAS-3** shows that the binding mode of the ligand is very similar in both complexes. As shown in Supplementary Figure S1, the chloride ion of the SAM-binding site interacts with the charged residues D53, D156, D280, K203, and K287. The side chain of K287 residue is stabilized by a hydrogen bond with the carboxylate group of D53 side chain, and thus the K287L mutation destroys this essential interaction and explains the decreased activity seen in this mutant.

FIDAS Agents Inhibit MAT2A Activity in SAM Synthesis. The biological function of MAT2A is the synthesis of SAM (Figure 4A), an obligate methyl donor in many methyltransferase reactions. Following methyl donation, SAM is converted to *S*-adenosylhomocysteine (SAH) (Figure 4A). To test if the FIDAS agents inhibit the enzymatic activity of MAT2A, we developed an *in vitro* method for the synthesis of SAM from L-methionine and ATP. SAM and SAH levels were determined by LC−MS/MS. We found that **FIDAS-3** inhibited SAM synthesis *in vitro* (Figure 4B). To determine the effects on SAM and SAH levels in CRC cells, we treated LS174T cells with **FIDAS-3** and **FIDAS-5**. SAM and SAH levels were again analyzed by LC−MS/MS (Supplementary Figure S2A). We found that the FIDAS agents reduced the levels of both SAM and SAH (Figure 4C and D). These data suggested that FIDAS analogues interact with MAT2A and inhibit MAT2A activity in

dx.doi.org/10.1021/cb3005353 | *ACS Chem. Biol.* 2013, 8, 796−803

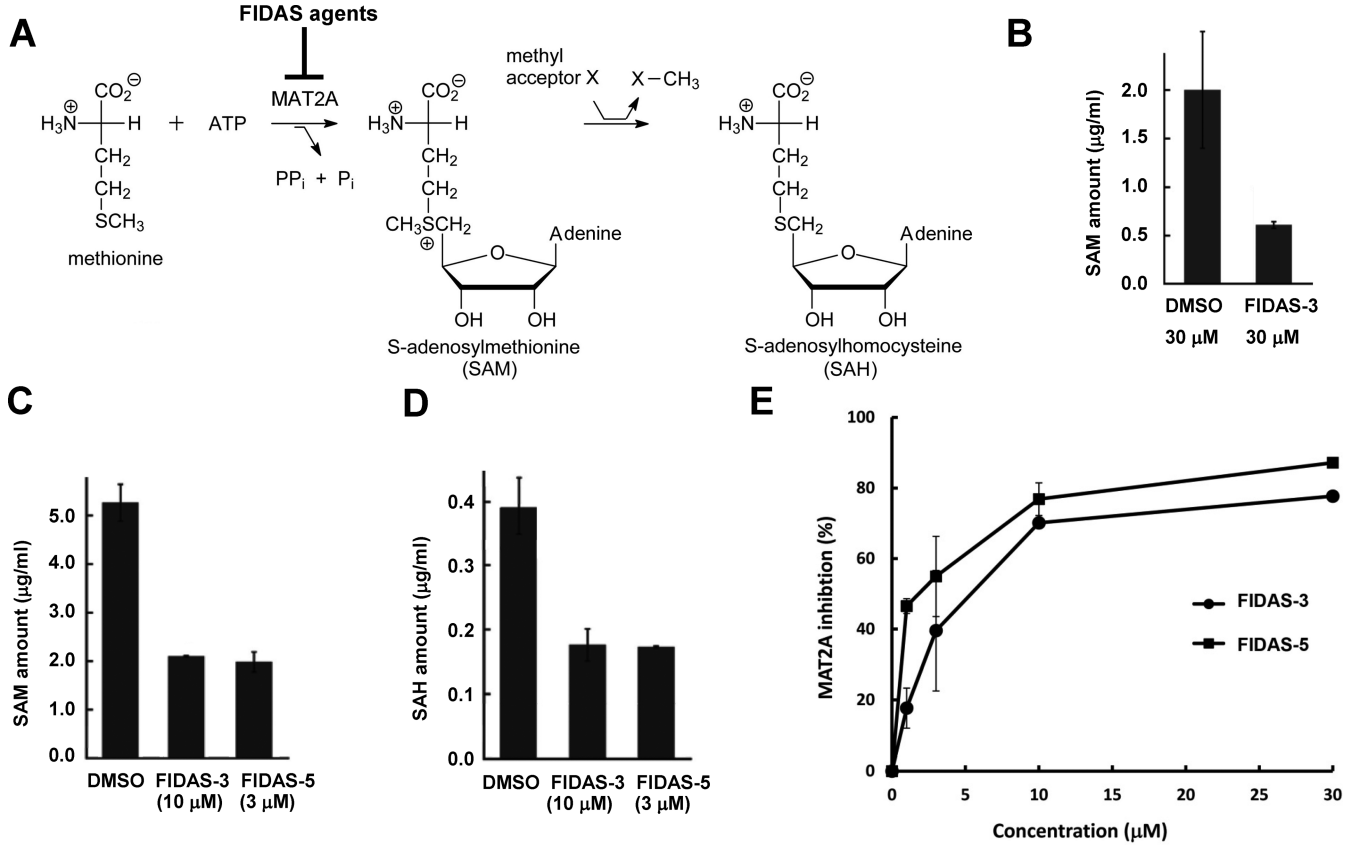

Figure 4. FIDAS analogues inhibited MAT2A activity. (A) Synthesis and function of *S*-adenosylmethionine (SAM). SAM is synthesized by MAT2A and is a major methyl donor for many methyltransferases. Subsequently, SAM is converted to *S*-adenosyl homocysteine (SAH) after the methyltransferase reaction. (B) **FIDAS-3** inhibited SAM synthesis *in vitro*. SAM was synthesized from L-methionine and ATP by purified MAT2A with or without **FIDAS-3**. SAM concentrations were measured by HPLC−MS/MS. (C and D) LS174T CRC cells were treated with **FIDAS-3** and **FIDAS-5** for 36 h. The levels of SAM and SAH were measure by HPLC−MS/MS. The SAM and SAH concentrations in the final solution for HPLC analysis are as indicated. (E) Dose-dependency analysis of MAT2A inhibition by **FIDAS-3 and FIDAS-5**. The assay was quantification of P_i using the Malachite Green assay. Presented data are means ± SD from 3 independent experiments.

SAM synthesis. To compare the activity of FIDAS agents on MAT2A inhibition, we performed an *in vitro* MAT2A assay in the presence of different doses of FIDAS agents. The product of MAT2A (P_i in Figure 4A) was analyzed by the Malachite Green method. We found that **FIDAS-5** is more potent than **FIDAS-3** in MAT2A inhibition (Figure 4E). The IC_{50}'s for **FIDAS-3** and **FIDAS-5** are around 4.9 and 2.1 μM, respectively. We also tested the effects of FIDAS agents *in vivo*. Mice were treated with either **FIDAS-5** (20 mg/kg) or the control vehicle (PEG400) for 1 week. The liver SAM levels were significantly reduced after FIDAS treatment (Supplementary Figure S2B).

MAT2A Is a Potential Target for CRC Treatment. To examine the role of MAT2A in CRC cell growth, we depleted MAT2A in CRC cells using shRNAs. MAT2A depletion reduced c-Myc expression (Figure 5A) and significantly inhibited the proliferation of LS174T CRC cells (Figure 5B). MAT2A shRNAs also inhibited the proliferation of other CRC cell lines, including HT29 (Figure 5C). These results are consistent with the function of FIDAS agents in CRC cells (Figure 1). Previously, we have shown that intraperitoneal injection of **FIDAS-3** in corn oil repressed the growth of LS174T CRC xenografts in athymic nude mice.[4] **FIDAS-5** is more potent than **FIDAS-3** in cell-based assays. In this study, we tested the oral efficacy of **FIDAS-5** on HT29 tumor xenografts in nude mice. Tumors were induced in athymic nude mice by subcutaneous injection of HT29 CRC cells. FIDAS treatment (20 mg/kg) or control vehicle was delivered orally by gavage. This dose was based on our previous studies with **FIDAS-3**.[4] Both groups were weighed (Figure 5D), and the tumors were measured twice weekly, using digital calipers. **FIDAS-5** significantly inhibited the growth of xenograft tumors (Figure 5E), with minimal difference in body weight (Figure 5D), as we have observed for **FIDAS-3**.[4] These results suggested that FIDAS agents are orally available for CRC treatment.

Stilbene-based natural products activate or repress a wide variety of cellular proteins, ligands, inflammatory agents, oncogenes, and tumor suppressors.[15] Our previous studies also found that FIDAS agents inhibited the Wnt pathway, and we now understand that the direct target of FIDAS agents is MAT2A. Since FIDAS agents inhibit the synthesis of SAM, which is required for methyltransferase activity, we hypothesize that the FIDAS agents may inhibit histone methylation required for gene activation, including the activation of Wnt target genes.[16] Other than protein methylation, SAM is also required for DNA methylation. Many tumor suppressor genes are inhibited by promoter methylation in cancer cells.[17] In addition, SAM regulates several important metabolic pathways arising out of the SAM cycle such as polyamine synthesis and transmethylation. SAM is also important for DNA synthesis. Although we only identified MAT2A/2B in this study, we

dx.doi.org/10.1021/cb3005353 | *ACS Chem. Biol.* 2013, 8, 796−803

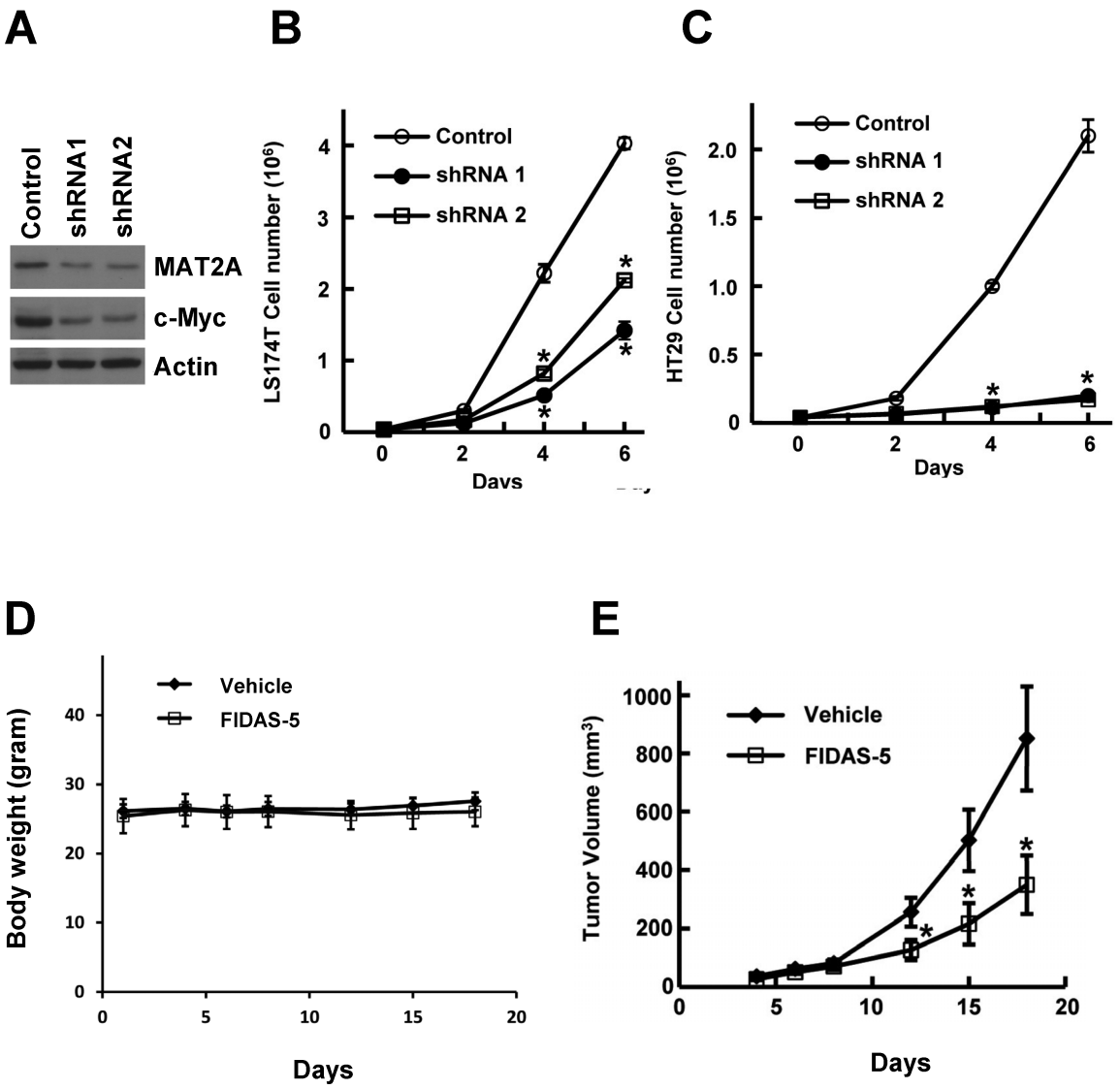

Figure 5. Inhibition of MAT2A repressed CRC cell growth *in vitro* and *in vivo*. (A) Effects of MAT2A shRNAs in LS174T CRC cells. (B) MAT2A shRNAs inhibited proliferation of LS174T CRC cells. Presented data are means ± SD from 3 independent experiments. (C) MAT2A shRNAs inhibited proliferation of HT29 CRC cells. Presented data are means ± SD from 3 independent experiments. (D and E) **FIDAS-5** inhibited the growth of xenograted HT29 cells in nude mice. HT29 cells (2×10^6) were injected subcutaneously into the flanks of athymic nude mice ($n = 16$). After 4 days, the mice were randomized into two groups. One group ($n = 8$) was treated with **FIDAS-5** (20 mg/kg/day) dissolved in PEG400 by gavage. The control mice ($n = 8$) were treated with the same volume of PEG400. The mice were weighed and tumors measured twice weekly for 2 weeks.

cannot rule out the possibility that FIDAS agents may also bind other target(s) directly or indirectly at higher concentrations than those studied here or in other cells than the ones used here. For example, MAT2B knockdown by shRNAs also inhibited the growth of colon cancer cells and liver cancer cells (Supplementary Figures S3 and S4A). In addition, many natural stilbenes may repress tumor cell growth through different mechanisms than the MAT2A inhibition reported here. Thus, FIDAS agents may repress tumor growth by multiple mechanisms, and we are actively exploring these possibilities.

In summary, we developed a novel family of stilbenes analogues, the FIDAS agents, by optimizing their anticancer activity. Our studies, as reported here, provide convincing evidence that the direct target of FIDAS analogues is MAT2A, specifically, the catalytic subunit responsible for the synthesis of SAM. MAT2A levels are significantly increased in CRC and liver cancers,[7−9] suggesting that MAT2A is a potentially interesting target for these cancers. We also analyzed the effects of FIDAS agents on other cancer cells (Supplenetary Figures S4B and S5) and found that these agents can inhibit the growth of multiple human cancer cell lines, including breast, prostate, lung, liver, carcinoid, and head and neck cancer cells. Our finding that FIDAS agents affect SAM synthesis that in turn plays such a central role in numerous biological processes suggests an important mechanism that can be exploited for cancer treatment. The FIDAS agents, which uniquely block the activity of the catalytic subunit of MAT2A, are promising lead candidates and great experimental tools to study the role of MAT2A inhibition in cancer therapy.

METHODS

Chemistry. Chemicals were purchased from Sigma Aldrich or Thermo Scientific or were synthesized according to literature

dx.doi.org/10.1021/cb3005353 | *ACS Chem. Biol.* 2013, 8, 796−803

procedures. Solvents were used from commercial vendors without further purification unless otherwise noted. Nuclear magnetic resonance spectra were determined on a Varian instrument (^{1}H, 400 MHz; ^{13}C, 100 Mz). LRMS electron-impact (EI) ionization mass spectra were recorded at 70 eV on a ThermoFinnigan PolarisQ (ion trap mass spectrometer). Samples were introduced via a heatable direct probe inlet. High resolution electron impact (EI) ionization mass spectra were recorded at 25 eV on a JEOL JMS-700T MStation (magnetic sector instrument) at a resolution of greater than 10,000. Samples were introduced *via* heatable direct probe inlet. Perfluorokerosene (pfk) was used to produce reference masses. MALDI mass spectra were obtained on a Bruker Utraflexstreme time-of-flight mass spectrometer (Billerica, MA), using DHB (2,5-dihydroxybenzoic acid) matrix. Purity of compounds was >95% as established by combustion analyses. In the case of compounds that resisted crystallization or were too valuable to sacrifice to combustion, purity was established by a combination of high resolution mass spectra and ^{13}C NMR data. Elemental analyses were determined by Atlantic Microlabs, Inc., Norcross, GA. Compounds were chromatographed on preparative layer Merck silica gel F254 unless otherwise indicated. Detailed methodology for chemical synthesis is described in Supporting Information.

Affinity Binding Assays. *LS174T Cell Lysates.* To purify the FIDAS target, LS174T cell lysates were incubated with streptavidin beads and biotinylated **FIDAS-8** at 4 °C overnight. The beads were washed three times with cell lysis buffer. Binding proteins were elution with 2.5 mM D-biotin. The purified samples were separated by 4−12% gradient SDS-PAGE and analyzed by silver staining or Sypro Ruby fluorescent staining. The protein bands specifically presented in the samples of **FIDAS-8** were excised and analyzed by MALDI-TOF/TOF and LC−MS/MS as previously described.[18]

Recombinant MAT2A. MAT2A and MAT2B were cloned into pGEX-6P-3 vector. The constructs were transfected into *E. coli* BL21. The GST-fusion proteins were induced by IPTG and purified by glutathione beads as described previously.[19] For the binding assay, purified proteins were incubated with streptavidin beads and the biotinylated **FIDAS-8** compound described above. Eluted proteins were analyzed by Western blotting with antibodies against GST, MAT2A, or MAT2B. His-tagged MAT2A was expressed from the pETDuet vector for use in SAM synthesis and mutagenesis studies. Protein was purified using HIS-Select resin (Sigma-Aldrich) according to manufactures instructions and eluted using buffer supplemented with 300 mM imidazole.

SAM Quantification. For *in vitro* synthesis assay, purified His-tagged MAT2A (5 μg) was incubated with 1 mM L-methionine and 1 mM ATP in 500 μL of reaction buffer. After incubation for 5 min at 25 °C, perchloric acid was added to quench the reaction and precipitate the protein. For cell-based assay, LS174T cells were cultured in RPMI1640 medium containing 5% FBS. Cells were treated with FIDAS agents for 36 h and then harvested and weighed. Perchloric acid (0.4 M) was added to the cell pellet (100 μL/30 mg) for deproteinization. For *in vivo* studies, perchloric acid (0.4 M) was added to liver tissues (100 μL/30 mg) and homogenized for deproteinization. The samples were mixed vigorously and centrifuged at 10,000*g*. Supernatant (60 μL) was mixed with 20 μL of an internal standard (5 μg/mL of SAH-d_4). The sample was adjusted to pH 5−7 with 2.5 M K_2HPO_4 and kept on ice for 15 min to precipitate potassium perchlorate. Samples were centrifuged twice at 10,000*g* for 15 min. Supernatants (5 μL of each sample) were analyzed by LC−MS/MS according to modified protocol.[20] SAM and SAH standard were prepared by serial dilutions with 0.4 M perchloric acid (PCA); the individual calibration points were 0.05, 0.5, 5, 50 μg/mL.

The LC−MS/MS system consisted of two Varian ProStar 210 LC pumps coupled with a Varian 1200L triple quadrupole mass spectrometer. The separation was performed on a Hypercarb column (50 mm × 2.1 mm, 3 mm, Thermo Scientific no. 35003-052130). Gradient elution started with 98% solution A (0.1% formic acid in water), followed by an increase to 38% solution B (0.1% formic acid in acetonitrile) in 8 min. The column was than washed with 90% B for 5 min and reconditioned with 98% A for another 8 min. The flow rate was 0.25 mL/min. Between the third and 11th min, the eluent was switched to the ion source of the mass spectrometer. The precursor product transitions for SAM (m/z 399→250), SAH (m/z 385→250), and SAH-d_4 (m/z 389→136) were monitored. The optimized ion source parameters were capillary voltage, 32 V for both SAM and SAH; collision energy, 9 and 7 V for SAM and SAH, respectively; needle voltage, 5000 V; and the shield voltage, 600 V. Nitrogen was used as the drying gas at a temperature of 300 °C, and the interface heater was set to 50 °C. The drying gas and nebulizing gas were set to 20 and 50 psi, respectively.

Anisotropy Analysis. FIDAS-3 (2.5 μM) was mixed with DMSO or MAT2A in 100 μL of PBS buffer in a 96-well plate. For competition assay, SAM or L-methionine was added to the mixture. Fluorescence anisotropy was measured at 23 °C using a SpectraMax M5 (Molecular Devices, Sunnyvale, CA) with excitation at 358 nm, emission at 454 nm, and an emission filter at 420 nm. Samples were measured in a colored 96-well plate with 100 μL total volume.

Malachite Green Phosphate (P_i) Assay. L-Methionine (1 mM) and ATP (1 mM) were incubated with purified His-tagged MAT2A (5 μg) in 0.5 mL of reaction buffer (50 mM Tris pH8.0, 50 mM KCl, 10 mL $MgCl_2$) for 30 min. The inorganic phosphate released from the reaction was measured with SensoLyte MG phosphate assay kit (AnaSpec, 71103). The absorbance was measured at 620 nm on a microplate reader (Spectra MR, DYNEX technologies). For inhibition assay, MAT2A was incubated with FIDAS agents at RT for 20 min and then mixed with L-methionine and ATP in 0.5 mL of reaction buffer. Cold deionized water (2 mL) was added to stop the reaction and dilute the samples.

Cell-Based Assays. *Western Blotting.* The activity of FIDAS agents on gene expression in cancer cells were analyzed by Western blotting with antibodies against β-Actin (Sigma-Aldrich), c-Myc (Epitomics, Inc.), Cyclin D1 (Epitomics, Inc.), and $p21^{WAF1/CIP1}$ (Cell Signaling Technology, Inc.). These antibodies have been described in our previous publication.[4] MAT2A and MAT2B antibodies were purchased from GeneTex.

Cell Proliferation. The cancer cells were plated into 12-well plates (4000 cells/mL). Next day, the cells were treated with FIDAS agents. The effects of FIDAS agents on cancer cell growth were analyzed using a Cell Viability Analyzer (Beckman Coulter, Vi-Cell XR). This assay has been described in a previous publication.[4]

shRNA Assay. ShRNA constructs for MAT2A and MAT2B were ordered from Sigma. HEK293T cells were transfected with lentivirus packaging plasmids psPAX2 and pMD2.G, as well as control or MAT2A/2B shRNA plasmids. Lentivirus stock was collected 48 h after transfection. HT29 and LS174T lines were infected by the lentivirus stock for 12 h, followed by sustained growth in fresh medium for 36−48 h. Infected cell lines were seeded in 12-well plate for proliferation assay. shRNA efficiency was tested by Western blotting using lysates from HEK293T cells cotransfected with pcDNA3.1-MAT2A and pLKO.1-shRNA plasmids or CRC cells transfected with shRNAs.

Tumor Xenograft in Nude Mice. HT29 CRC cells (2×10^6) were subcutaneously injected into the flanks of 16 athymic nude mice. After 4 days, the mice were randomized into two groups. One group (n = 8) was treated with **FIDAS-5** (20 mg/kg/day) dissolved in PEG400 by gavage. The control group (n = 8) was treated with the same volume of PEG400. The mice were weighed and tumors measured twice weekly for 2 weeks as described previously.[4]

Molecular Modeling. To explore the possible MAT2A-**FIDAS-3** binding mode, the **FIDAS-3** ligand was docked to the dimeric MAT2A structure (PDB code: 2P02). The molecular docking and MD simulations were performed in the same way as we reported previously for other protein−ligand systems.[21−23] Detailed methods are described in the Supporting Information.

■ ASSOCIATED CONTENT

Supporting Information

This material is available free of charge via the Internet at http://pubs.acs.org

AUTHOR INFORMATION

Corresponding Author

*E-mail: chunming.liu@uky.edu.

Author Contributions

[¶]These authors contribute equally to this work.

Notes

The authors declare the following competing financial interest(s): D.S.W., C.L., V.S., and W.Z. are inventors of FIDAS agents (U.S. Patent 20120196874).

ACKNOWLEDGMENTS

We thank J. Thorson for suggestions and J. May, S. Singh, J. Goodman, H. Zhu, and P. Rychahou for technical assistance. C.L. was supported by R01 DK071976 and R21 CA139359 from the National Institutes of Health. B.M.E. was supported by UK SPORE grant (P20 CA 150343) and R01 DK048498. D.S.W. was supported by a grant from the National Center for Research Resources (5P20RR020171-09) and the National Institute of General Medical Sciences (8 P20 GM103486-09) from the National Institutes of Health.

REFERENCES

(1) ACS (2011) Colorectal cancer facts and figures 2011−2013, American Cancer Society, Atlanta.

(2) Hope, C., Planutis, K., Planutiene, M., Moyer, M. P., Johal, K. S., Woo, J., Santoso, C., Hanson, J. A., and Holcombe, R. F. (2008) Low concentrations of resveratrol inhibit Wnt signal throughput in colon-derived cells: implications for colon cancer prevention. *Mol. Nutr. Food Res. 52* (Suppl 1), S52−61.

(3) Paul, S., DeCastro, A. J., Lee, H. J., Smolarek, A. K., So, J. Y., Simi, B., Wang, C. X., Zhou, R., Rimando, A. M., and Suh, N. (2010) Dietary intake of pterostilbene, a constituent of blueberries, inhibits the beta-catenin/p65 downstream signaling pathway and colon carcinogenesis in rats. *Carcinogenesis 31*, 1272−1278.

(4) Zhang, W., Sviripa, V., Kril, L. M., Chen, X., Yu, T., Shi, J., Rychahou, P., Evers, B. M., Watt, D. S., and Liu, C. (2011) Fluorinated N,N-dialkylaminostilbenes for wnt pathway inhibition and colon cancer repression. *J. Med. Chem. 54*, 1288−1297.

(5) Cantoni, G. L. (1953) S-Adenosylmethionine; a new intermediate formed enzymatically from L-methionine and adenosinetriphosphate. *J. Biol. Chem. 204*, 403−416.

(6) Lu, S. C., and Mato, J. M. (2008) S-Adenosylmethionine in cell growth, apoptosis and liver cancer. *J. Gastroenterol. Hepatol. 23* (Suppl 1), S73−77.

(7) Cai, J., Sun, W. M., Hwang, J. J., Stain, S. C., and Lu, S. C. (1996) Changes in S-adenosylmethionine synthetase in human liver cancer: molecular characterization and significance. *Hepatology 24*, 1090−1097.

(8) Chen, H., Xia, M., Lin, M., Yang, H., Kuhlenkamp, J., Li, T., Sodir, N. M., Chen, Y. H., Josef-Lenz, H., Laird, P. W., Clarke, S., Mato, J. M., and Lu, S. C. (2007) Role of methionine adenosyltransferase 2A and S-adenosylmethionine in mitogen-induced growth of human colon cancer cells. *Gastroenterology 133*, 207−218.

(9) Ito, K., Ikeda, S., Kojima, N., Miura, M., Shimizu-Saito, K., Yamaguchi, I., Katsuyama, I., Sanada, K., Iwai, T., Senoo, H., and Horikawa, S. (2000) Correlation between the expression of methionine adenosyltransferase and the stages of human colorectal carcinoma. *Surg. Today 30*, 706−710.

(10) Yu, T., Chen, X., Zhang, W., Colon, D., Shi, J., Napier, D., Rychahou, P., Lu, W., Lee, E. Y., Weiss, H. L., Evers, B. M., and Liu, C. (2011) Regulation of the potential marker for intestinal cells, Bmi1, by beta-catenin and the zinc finger protein KLF4: Implications for colon cancer. *J. Biol. Chem. 287*, 3760−3768.

(11) Lin, H., Sviripa, V., Watt, D. S., Liu, C., Xiang, T., Anderson, B. D., Ong, P. S., and Ho, P. C. (2013) Quantification of *trans*-2,6-difluoro-4′-N,N-dimethylaminostilbene in rat plasma: Application to a pharmacokinetic study. *J. Pharm. Biomed. Anal. 72*, 115−120.

(12) Gonzalez, B., Pajares, M. A., Hermoso, J. A., Guillerm, D., Guillerm, G., and Sanz-Aparicio, J. (2003) Crystal structures of methionine adenosyltransferase complexed with substrates and products reveal the methionine-ATP recognition and give insights into the catalytic mechanism. *J. Mol. Biol. 331*, 407−416.

(13) Komoto, J., Yamada, T., Takata, Y., Markham, G. D., and Takusagawa, F. (2004) Crystal structure of the S-adenosylmethionine synthetase ternary complex: a novel catalytic mechanism of S-adenosylmethionine synthesis from ATP and Met. *Biochemistry 43*, 1821−1831.

(14) Finkelstein, J. D. (1990) Methionine metabolism in mammals. *J. Nutr. Biochem. 1*, 228−237.

(15) Chachay, V. S., Kirkpatrick, C. M., Hickman, I. J., Ferguson, M., Prins, J. B., and Martin, J. H. (2011) Resveratrol−pills to replace a healthy diet? *Br. J. Clin. Pharmacol. 72*, 27−38.

(16) Sierra, J., Yoshida, T., Joazeiro, C. A., and Jones, K. A. (2006) The APC tumor suppressor counteracts beta-catenin activation and H3K4 methylation at Wnt target genes. *Genes Dev. 20*, 586−600.

(17) Ying, Y., and Tao, Q. (2009) Epigenetic disruption of the WNT/beta-catenin signaling pathway in human cancers. *Epigenetics 4*, 307−312.

(18) Zhang, W., Chen, X., Kato, Y., Evans, P. M., Yuan, S., Yang, J., Rychahou, P. G., Yang, V. W., He, X., Evers, B. M., and Liu, C. (2006) Novel cross talk of Kruppel-like factor 4 and beta-catenin regulates normal intestinal homeostasis and tumor repression. *Mol. Cell. Biol. 26*, 2055−2064.

(19) Liu, C., Kato, Y., Zhang, Z., Do, V. M., Yankner, B. A., and He, X. (1999) beta-Trcp couples beta-catenin phosphorylation-degradation and regulates Xenopus axis formation. *Proc. Natl. Acad. Sci. U.S.A. 96*, 6273−6278.

(20) Gellekink, H., van Oppenraaij-Emmerzaal, D., van Rooij, A., Struys, E. A., den Heijer, M., and Blom, H. J. (2005) Stable-isotope dilution liquid chromatography-electrospray injection tandem mass spectrometry method for fast, selective measurement of S-adenosylmethionine and S-adenosylhomocysteine in plasma. *Clin. Chem. 51*, 1487−1492.

(21) Bargagna-Mohan, P., Hamza, A., Kim, Y. E., Khuan Abby, Ho, Y., Mor-Vaknin, N., Wendschlag, N., Liu, J., Evans, R. M., Markovitz, D. M., Zhan, C. G., Kim, K. B., and Mohan, R. (2007) The tumor inhibitor and antiangiogenic agent withaferin A targets the intermediate filament protein vimentin. *Chem. Biol. 14*, 623−634.

(22) Bargagna-Mohan, P., Paranthan, R. R., Hamza, A., Dimova, N., Trucchi, B., Srinivasan, C., Elliott, G. I., Zhan, C. G., Lau, D. L., Zhu, H., Kasahara, K., Inagaki, M., Cambi, F., and Mohan, R. (2010) Withaferin A targets intermediate filaments glial fibrillary acidic protein and vimentin in a model of retinal gliosis. *J. Biol. Chem. 285*, 7657−7669.

(23) Zhou, M., Hou, Y., Hamza, A., Zhan, C. G., Bugni, T. S., and Thorson, J. S. (2012) Probing the regiospecificity of enzyme-catalyzed steroid glycosylation. *Org. Lett. 14*, 5424−5427.